

# Velocity Profiles of Boron Atoms Sputtered from Boron Nitride by Low Energy Xenon Ions

IEPC-2011-067

Presented at the 32nd International Electric Propulsion Conference,  
Wiesbaden • Germany  
September 11 – 15, 2011

Lei Tao<sup>1</sup>, Azer Yalin<sup>2</sup>  
Colorado State University, Fort Collins, CO, 80523, USA

**Abstract:** Details of the boron nitride (BN) sputtering process at low ion energies are of interest for diagnostics and modeling of Hall thruster erosion. This contribution presents velocity distributions of sputtered boron atoms from BN targets due to low energy ions. The velocity distributions were found from laser induced fluorescence (LIF) spectroscopy of boron with a tunable diode laser system in the vicinity of 250 nm. Measurements were performed for normally incident xenon ions at energies in the range of 100-1200 eV. In addition, two measurements have been done for ion incidence angles of 60° and 45°. The LIF velocity profiles for sputtered boron from BN were fitted with Thompson distributions. A surface binding energy of  $E_b=4.8\pm 0.2$  eV for boron from BN was measured and showed little dependence on Xe ion energy.

## Nomenclature

$c$	=	speed of light
$E_b$	=	surface binding energy
$f$	=	focal length
$m$	=	energy-dependent parameter in Sigmund-Thompson distribution
$M$	=	atomic mass
$u$	=	velocity component of particles along the laser beam
$v_b$	=	corresponding atomic velocity for $E_b$
$Z$	=	the distance from the detection point to the target surface
$h\nu$	=	photon energy
$\nu_0$	=	resonance frequency
$\nu_L$	=	laser frequency
$\Delta\nu$	=	frequency shift of the fluorescence signal
$\lambda_0$	=	transition wavelength

## I. Introduction

Boron nitride (BN) is the most widely used material for the acceleration channel wall that protects the magnetic circuitry from the discharge plasma in a Hall thruster<sup>1-3</sup>. The major mechanism limiting the lifetime of Hall thrusters is sputter erosion of the BN wall due to bombarding of ion fluxes (~100 eV) having non-axial trajectories. Hall thruster reliability is critical for applications requiring prolonged operation. Currently, in procedures referred to as ground-based tests, Hall thrusters are operated beyond their expected total thrust duration in a vacuum chamber<sup>1-3</sup>. This is the primary method to verify sufficient life of a Hall thruster for its mission. The method allows only *post facto* analysis of the lifetime and becomes increasing impractical and expensive for proposed future thrusters with missions of 5-10+ years. It also provides limited understanding of the erosion mechanisms, for example the

<sup>1</sup> Graduate Research Associate, Mechanical Engineering, leitao@colostate.edu

<sup>2</sup> Associate Professor, Mechanical Engineering, ayalin@enr.colostate.edu

dependence of erosion rate on operation conditions. The low sputter erosion rates of BN combined with the need for *in situ* measurements severely limit the available diagnostic methods.

Ongoing research efforts at the Laser Plasma Diagnostics Laboratory (LPDL) at Colorado State University, in partnership with the Plasmadynamics and Electric Propulsion Lab at University of Michigan, are developing cavity ring-down spectroscopy (CRDS) sensors for electric propulsion applications, including erosion monitoring, as well as for industrial ion beam etch systems<sup>4-10</sup>. We have demonstrated the use of a CRDS sensor to monitor sputter eroded manganese from a steel channel within an anode layer thruster<sup>10</sup>. Furthermore, a CRDS sensor for *in situ* BN sputter erosion measurements has been developed for Hall thrusters and has been used to obtain a demonstrative spectrum of sputtered boron atoms from BN target<sup>9</sup>. Recent work has also shown initial CRDS detection of sputtered boron from the BN channel of a magnetic layer Hall thruster<sup>11</sup>.

CRDS directly measures the path-integrated number density of particles along the optical axis. However, computation of the corresponding BN erosion rate requires the flux density of the sputtered particles, which depends on both the number density and velocity of sputtered particles. Therefore, the velocity (distribution) of sputtered boron atoms (from BN materials) is a critical parameter for interpretation of measurements from BN CRDS erosion sensors. While ejection velocities and binding energies are generally known for single-component targets, the situation is more difficult for multi-component targets. Our past work has, to the best of our knowledge, provided the first velocity measurements of boron from sputtered BN targets<sup>12</sup>. Additionally, velocity spectra of sputtered atoms give direct and detailed insight into the basic sputtering mechanism<sup>13</sup>. The velocity (energy) distribution of sputtered boron allows determination of the surface binding energy  $E_B$  and, when combined with angular (differential) sputter yield data, provides a rich description of the BN sputtering process. For these reasons, velocity measurements of sputtered boron from BN targets are needed in Hall thruster research.

In this paper, we report LIF measurements of velocity distributions of sputtered boron atoms due to low energy ion beam bombardment of a BN target. The present contribution thus extends our previous research<sup>12</sup>. The LIF technique provides *in situ* non-intrusive velocity resolved measurements. Similar experiments for sputtered boron atoms from different materials have been done for applications in fusion<sup>14-16</sup>. We follow their approach including the use of opto-galvanic spectroscopy to provide a frequency reference for the LIF measurements. The layout of this paper is as follows. The diagnostic technique and experimental apparatus are described in Section II. The analysis of experimental results is presented in Section III. Finally, in Section IV, we present conclusions.

## II. Experimental

### A. LIF Measurement of Velocity Distribution

LIF is widely used technique for non-intrusive velocity distribution measurements of sputtered atoms or molecules vacuum (collisionless) conditions<sup>12-19</sup>. A tunable laser with frequency  $\nu_L$  illuminates the targeted species. The transition frequency of a stationary atom is  $\nu_0$ , whereas the atoms with a velocity component  $u$  away from (and parallel to) a laser beam can only absorb photons if they satisfy the Doppler shift condition. The magnitude of frequency shift  $\Delta\nu$  is:

$$\Delta\nu = \nu_L - \nu_0 = \frac{u}{c} \nu_0 \quad (1)$$

The subsequent fluorescence emission from excited atoms is detected and recorded as a function of the laser frequency. By scanning a laser near a known transition, the wavelength distribution of the fluorescence intensity is broadened based on the velocity distribution of the absorbing species along the path of the laser. Note that owing to the collisionless environment, thermal and pressure broadenings do not come into play. Thus the velocity distribution can be derived from the fluorescence spectrum. Figure 1 shows the selected boron atomic transition line and the fluorescence signal. The ground state for this species has two distinct levels:  $2p^2P_{1/2}$  (at 0 eV) and  $2p^2P_{3/2}$  (at 0.00189 eV). In this work, boron atoms were pumped from ground state  $2p^2P_{3/2}$  to excited state  $3s^2S_{1/2}$  by a laser at  $\lambda_0 = 249.8$  nm. The fluorescence signal comes from the de-excitation of the excited atoms with a radiative lifetimes of 4 ns<sup>20</sup>.

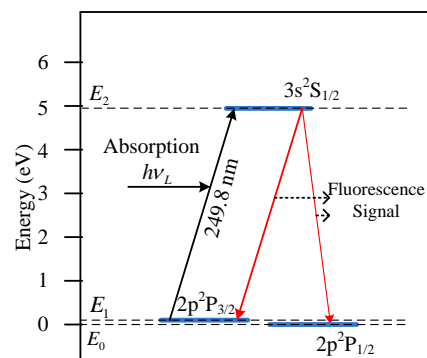
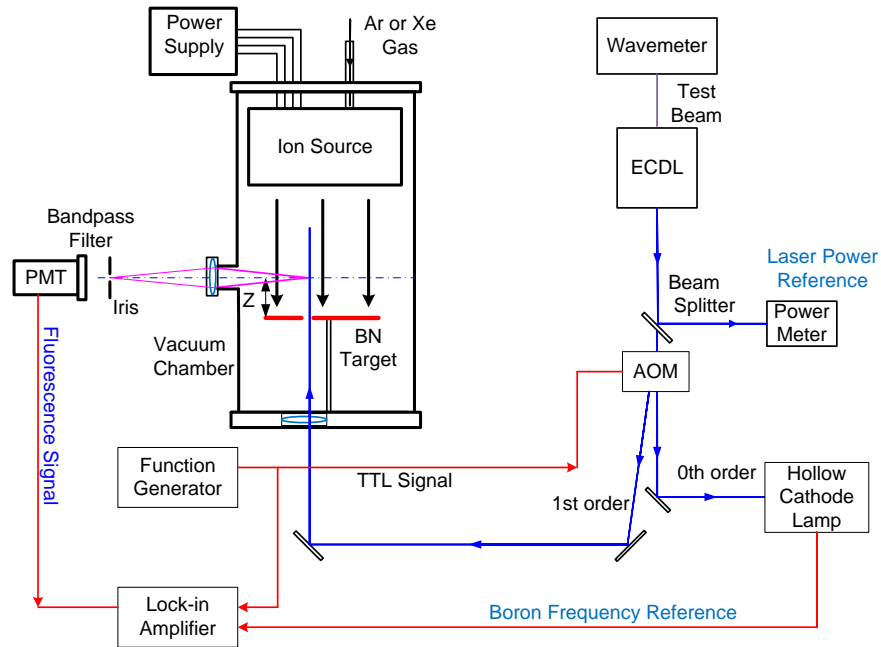


Figure 1. Selected boron transitional

## B. Apparatus

The tunable laser used to excite sputtered boron atoms was a frequency-quadrupled external cavity diode laser (ECDL) system (Toptica TA-FHG110) with  $\sim 10$  mW power output and  $\sim 5$  MHz linewidth. The ECDL system used a  $1 \mu\text{m}$  laser diode as the laser source. The  $1 \mu\text{m}$  laser beam was amplified by a tapered amplifier and then passed through two (actively locked) frequency-doubling cavities. A test beam at  $1 \mu\text{m}$  from the ECDL system was used along with a wavemeter (Coherent Wavemaster) to check the frequency (wavelength) of the laser. The laser frequency measurement resolution was 0.1 GHz which corresponds to a resolution of 0.4 GHz (100 m/s) for the 250 nm UV beam. The absolute frequency (“zero” of the distribution) was also checked with a hollow cathode lamp (HCL) as will be described below. The UV laser beam was capable of continuously tuning approximately 150 GHz around  $\lambda_0$  by changing both the voltage of the piezo-electric stack in the external cavity and the temperature of the laser diode. In the present experiments, the laser was manually tuned to scan through the targeted wavelength range (at a series of discrete wavelength steps). During the scan, the output power was monitored and adjusted to maintain a constant level.



**Figure 2. Experimental setup for boron LIF measurements.**

Figure 2 shows a diagram of the experimental set-up for boron LIF measurements. The sputtering test bed was housed in a vacuum chamber, where roughing and turbo pumps (Turbo-V550) were used to bring the pressure to approximately 0.1 mPa under no-flow conditions and to approximately 1 mPa under a small feeding flow for the ion source. At these conditions, the sputtered atoms were in a free-molecular regime (Knudsen number  $\ll 1$ ). A Kaufman type ion source generated an ion beam to bombard the target and produce sputtered particles. The ion source operated with an IonTech power supply (MPS 3000), with typical beam currents and voltages of about 10-40 mA and 100-1200 V respectively. High-purity argon (Ar) and xenon (Xe) gases were used as the working gas with thermal mass-flow controllers. The ion beam was normally incident upon the target. A 14 mm by 14 mm sputter target with a  $\sim 4$  mm diameter center bore for the beam to pass through was held by an adjustable post. In tests with non-normal incidence angles, the target was held on top of a wedged block. At the exit of the ECDL, a beam splitter directed  $\sim 10\%$  of the beam into a power meter to monitor the laser power output. The remainder of the beam was directed to an acousto-optic modulator (AOM) which was used as a fast optical switch and controlled by a function generator. The zero'th order beam from the AOM was directed to a commercial boron hollow cathode lamp (HCL) for frequency reference, whereas the first order beam was delivered into the vacuum chamber with a fused silica window and focused loosely in front of the target. The beam was carefully aligned and passed through a small circular hole in the target center to minimize the light scattering. The fluorescence light was collected by a 2.53 cm diameter fused silica lens with  $f=150$  mm at position  $Z=55$  mm above the target. The light was imaged onto a photomultiplier

tube (PMT, Hamamatsu R3896) with a dielectric interference filter (center wavelength at 250 nm and a transmission bandwidth of 30 nm). The PMT was operated at 1000 V with a 8 k $\Omega$  transimpedance resistor connected to its output.

When the ion source was on, there was strong background light from both the neutralizer filaments and the ion beam. On the other hand, BN has a low sputter yield and our laser has relatively low power, so that the resulting fluorescence signal was much weaker than the background noise (and undetectable). Initial measurements failed to detect the LIF signal against the strong light background. Therefore, a lock-in detection technique with a chopped laser beam was used to detect the fluorescence signal and improve the signal-to-noise ratio (SNR). A function generator produced a TTL square-wave signal to modulate the AOM to chop the laser beam at typical rates of 500 Hz. The PMT's voltage signal across the transimpedance resistor (30  $\mu$ V range) was filtered and amplified by a dual phase lock-in amplifier (EG&G 5210) with a reference TTL signal and a time constant of 10 s or 30 s. The lock-in time constant was selected to be slow enough to achieve high SNR. The use of the lock-in configuration resulted in a final SNR ratio of  $\sim$ 150 at high ion energy. However, the fluorescence signal decreases with decreasing ion energy, owing to diminished beam quality of the ion source and reduced sputter yield of the target. As a result, for the low ion energy tests ( $<$ 300 eV), we had poorer SNR due to competing background noise from scattering of the laser beam (which can be neither blocked by the filter in front of the PMT nor removed by the lock-in amplifier). Measures, such as using a light absorbent material for the beam dump, and implementing tube and irises, were taken to suppress the scattered light and increase SNR.

### C. Boron Reference Spectrum from Hollow Cathode Lamp

The LIF velocity measurements require accurate determination of the frequency shifts shown in Eq. (1) including properly locating the zero of the frequency axis (i.e. the frequency corresponding to stationary atoms). In this study, a reference spectrum of boron atoms was measured through the opto-galvanic effect and used to set (or "zero") the absolute frequency and velocity axes. The opto-galvanic technique can be considered as an alternative to absorption or fluorescence technique<sup>21</sup>. The opto-galvanic effect is observed as a perturbation in the conductivity of a self-sustained gaseous discharge, when the discharge is illuminated by radiation resonant with an atomic or molecular transition of the elements within it. It gives a simple and economical way to obtain an atomic or molecular spectrum and can be used in a wide range of applications including spectroscopy, small-concentration detection, isotopic analysis, laser calibration, and laser stabilization<sup>21</sup>. The pressure and mean free path of boron in the HCL ensure that its spectrum is centered at the zero velocity position.

A commercial hollow cathode lamp (HCL) with boron on the cathode provided a glow discharge of boron with an enlargement of the negative glow region. The HCL was filled with 133 Pa of Ne gas. When connected to a DC power supply, a gaseous discharge of Ne occurs within the HCL and produces Ne ions that bombard the cathode surface and sputter a portion of the cathode material (boron) to the gas phase. Figure 3 shows the detailed diagram of HCL setup. About 5 mW of laser power from the AOM was directed into the negative glow region of the HCL through a fused silica window. The HCL was operated at 6 mA of discharge current. Opto-galvanic signals were detected across the ballast resistor of 30 k $\Omega$  with a 0.47 mF capacitor. The lock-in amplifier filtered and amplified the signal. The beam (AOM) and lock-in were modulated with a TTL frequency reference signal from a function generator. A digital oscilloscope was used to record the signal. Modulation and lock-in parameters were similar to those used in the LIF experiments.

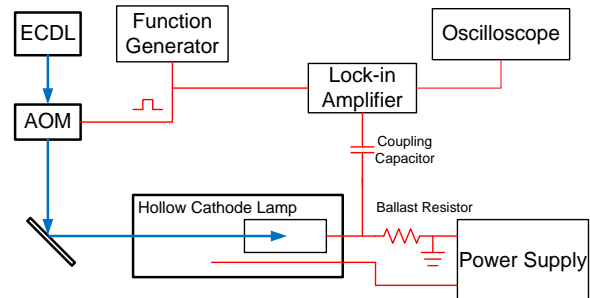


Figure 3. HCL frequency reference.

The sputtered boron from the BN target has a somewhat under-cosine angular distribution (differential sputter yield profile)<sup>21</sup>, but with a significant number of particles ejected normal to the target surface. The distance  $Z$  in the experiments was chosen to be much larger than the dimension of the target. As a result, the target can be considered a point source in the model for fitting the experimental data. The point source assumption is quite valid as a result of the small half apex angle ( $10^\circ$  maximum) from the detection point to the target boundary (giving at worst 98% alignment of the velocity vector with the optical axis). In this case, the (flux based) velocity distribution  $f(u)$  of sputtered boron atoms along the laser beam follows a Sigmund-Thompson distribution<sup>13,12</sup>:

### III. Results and Analysis

The sputtered boron from the BN target has a somewhat under-cosine angular distribution (differential sputter yield profile)<sup>21</sup>, but with a significant number of particles ejected normal to the target surface. The distance  $Z$  in the experiments was chosen to be much larger than the dimension of the target. As a result, the target can be considered a point source in the model for fitting the experimental data. The point source assumption is quite valid as a result of the small half apex angle ( $10^\circ$  maximum) from the detection point to the target boundary (giving at worst 98% alignment of the velocity vector with the optical axis). In this case, the (flux based) velocity distribution  $f(u)$  of sputtered boron atoms along the laser beam follows a Sigmund-Thompson distribution<sup>13,12</sup>:

$$f(u) \propto \frac{u^3}{(u^2 + v_b^2)^{3-2m}} \quad (2)$$

where  $v_b$  is the atomic velocity corresponding to  $E_b$  ( $\equiv Mv_b^2/2$ ), and  $m$  is an energy-dependent parameter in the differential cross-section relating to the screened Coulomb potential. Specification of the velocity distribution requires both  $m$  and  $v_b$  ( $E_b$ ). The value of  $m$  varies from approximately 0-0.3 for low ion energies ( $< \sim 1$  keV)<sup>13</sup>. In the present work, the measured profiles were fitted with  $m$  and  $v_b$  both as free parameters (least-squares method). The strong sensitivity to  $m$  is discussed below.

### A. Demonstrative Measurements

Prior to BN measurements, velocity profiles were performed for a pure boron target ( $\sim 99.9\%$  purity) to validate the experiment setup and method. Figure 4 shows the LIF spectrum from pure boron sputtered by an argon ion beam (1200 V, 30 mA) as well as the wavelength reference signal of the boron opto-galvanic HCL spectrum<sup>12</sup>. The HCL spectrum has a full width at half maximum of  $\sim 20$  GHz. The peak of the spectrum was used as the reference (“zero”) for the LIF spectra and was located within  $\pm 0.01$  GHz uncertainty (approximately 40 times better precision than is possible with our wavemeter for the UV beam). A Sigmund-Thompson profile, which best fits the experimental LIF curve, gives  $m=0\pm 0.02$  and  $v_b=10,000\pm 300$  m/s ( $E_b=5.7\pm 0.3$  eV). The error bars are based on 95% confidence bounds from fitting. The measured  $E_b$  agrees with the sublimation energy of boron (5.73 eV) from the computer code Srim and Trim<sup>22</sup> and the experimental result of Ito, Y. *et al.* (6 eV)<sup>16</sup>.

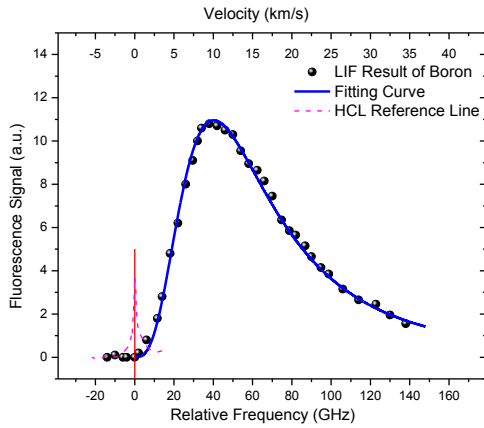


**Figure 4. Boron LIF spectrum and fit for Ar ions at 1200 eV.**

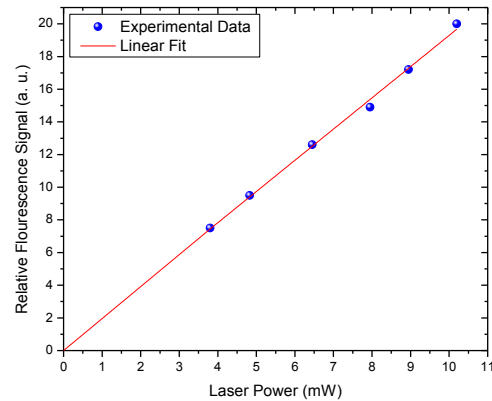


**Figure 5. LIF signal intensity versus illuminated laser power.**

The LIF velocity measurement should be performed in the linear regime, where the fluorescence signal is linearly proportional to the induced laser power. The input laser power of 250 nm was about 10 mW. The laser beam was focused to a beam diameter of 0.6 cm in front of the target. In a rough calculation, this gave the laser irradiance to be  $35$  W/cm<sup>2</sup>. Based on a zero quenching condition, the saturated laser irradiance was calculated to be  $0.64$  GW/cm<sup>2</sup> at the transition peak. Therefore, we expect the measurements are within the linear regime. An experimental validation of the linearity of the fluorescence signal strength has been performed by varying the illuminated laser power manually with an ion beam of 600 eV and 30 mA as shown in Fig. 5, while the laser frequency was kept constant with the absorption range of boron atoms. The experimental result of LIF signal was linearly proportional to the laser power with a linear correlation coefficient of 0.996, thus confirming the linear regime.

### B. BN LIF Spectra

The LIF spectra of sputtered boron from a BN target (grade HBR, obtained from GE Advanced Materials) have been measured with both Ar and Xe ions. Three tests were first done with an Ar ion beam at energies of 300, 800, and 1200 eV, all at current of 30 mA. The best fit values of  $m$  and  $v_b$  ( $E_b$ ) for all four measurement conditions are listed in Table 1. Figure 6 shows the three LIF spectra along with the corresponding fitted profiles. All values of  $m$  are close to 0.2 and in the expected range of 0-0.3 for low energy ions. It is noteworthy that there is a large influence

of  $m$  on the associated best fit value of  $v_b$ . To illustrate this, Figure 7 shows best fit profiles for the BN experimental data for 800 V Ar ion beam for different cases where  $m$  is fixed and  $v_b$  treated as the sole fit parameter. The best-fit values of  $v_b$  change from 11,300 m/s ( $E_b=7.2$  eV) to 8,200 m/s ( $E_b= 3.9$  eV) as  $m$  varies from 0 to 0.3.

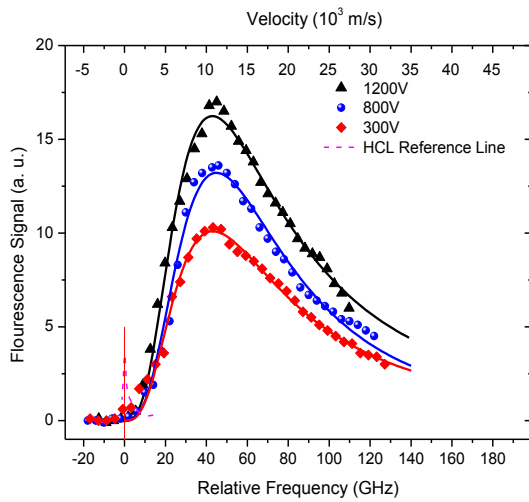


Figure 6. BN LIF spectra and fits at different Ar ion energies.

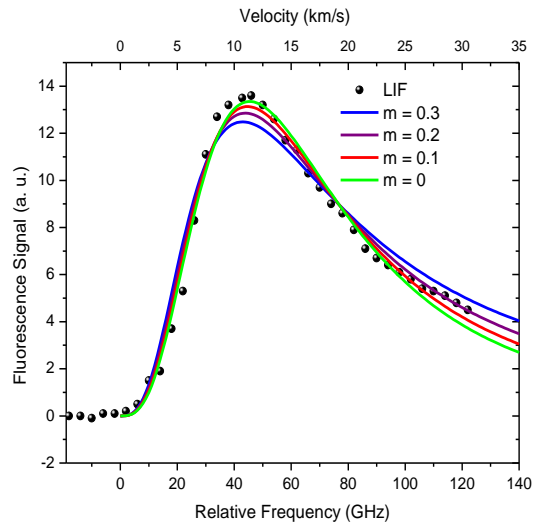


Figure 7. Best fit profiles for several values of  $m$  for Ar ions at 800 eV.

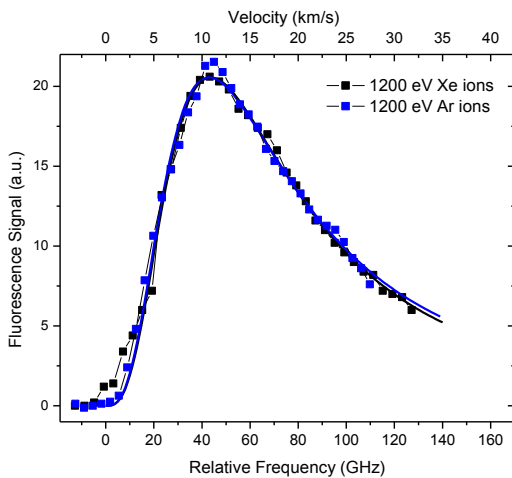


Figure 8. BN LIF spectra and fits for Xe and Ar ions at 1200 eV.

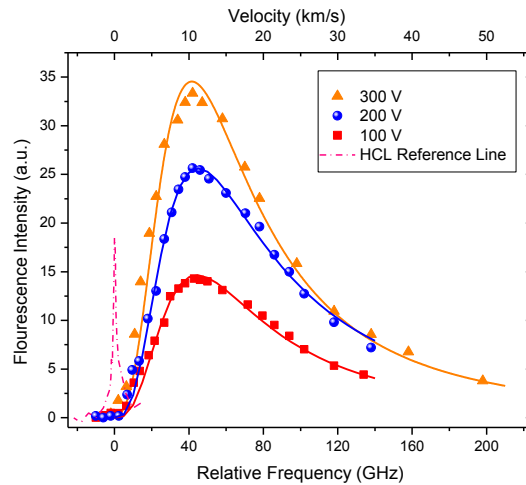


Figure 9. BN LIF spectra and fits at different Xe ion energies.

In Hall thrusters, the Xe ions that erode the BN wall material have typical average energy of  $\sim 100$  eV<sup>23</sup>, which may depend on the discharge voltage (normally 100 to 500 V). Therefore, the sputtered boron velocity distribution from low energy Xe ion is of most interest for Hall thrusters. All the results shown above were done with an Ar ion beam at relatively high energy. The simplest theoretical expectation is that the binding energy is material (target) dependent but does not (strongly) depend on the ion energy, species, or incidence angle<sup>13</sup>. In Fig. 8, the velocity distributions from the Ar ion beam test and a Xe ion beam test at 1200 V are shown together (after scaling of the ordinate axis). At these conditions, the profiles of sputtered boron atoms do not show strong dependence on the incident ion species.

Ar Ion beam condition	$m$	$v_b$ (m/s)	$E_b$ (eV)
300 V	0.20±0.04	9,200±300	4.8±0.3
800 V	0.19±0.02	9,200±400	4.8±0.4
1200 V	0.22±0.05	9,100±400	4.7±0.4

**Table 1. Best fit parameters for boron velocity profiles for sputtered BN as found from LIF.**

To investigate the low energy sputtering behavior, several tests were performed with a Xe ion beam at 100, 200, and 300 V. Figure 9 shows measured spectra and fits for these low energy Xe LIF experiments. In addition to the normal incident angle, two initial measurements were done with the ion beam at 45° and 60° incidence (relative to the target). In that case, the target was hold on top of a block with a wedged angle of 45° and 60°. Table 2 shows all the fitting results for Xe LIF experiments with  $m$  and  $V_b$  both as free parameters. The error bars were calculated based on 95% confidence bounds from fitting.

Xe Ion beam condition		$m$	$v_b$ (m/s)	$E_b$ (eV)
100V	Test1	0.23±0.04	9,000±500	4.5±0.6
	Test2	0.21±0.02	9,500±500	5.0±0.6
200V	Test1	0.24±0.02	9,200±300	4.8±0.3
	Test2	0.22±0.02	9,200±350	4.8±0.4
300V	Test1	0.20±0.03	9,100±350	4.6±0.4
	Test2	0.23±0.02	9,100±350	4.6±0.4
1200V	Test1	0.17±0.05	9,500±500	5.0±0.6
300V	45° incidence	0.21±0.03	8,700±500	4.3±0.4
	60° incidence	0.19±0.04	8,800±400	4.3±0.4

**Table 2. Fitting results for LIF measurements with Xe ion beam.**

The measured binding energies for boron (from BN target) for bombardment by Xe and Ar ions, at all conditions studied, are approximately constant with  $E_b=4.8±0.2$  eV (based on averaging the measured data). The average value of the  $m$  parameter is likewise found as  $m=0.22±0.04$ . It should be noted, however, that the error bars for the measurements with lower energy Xe ions are larger (as discussed above). Experimental results of non-normal incidence don't show strong angular dependence within the limited number of experiments. Some past research, with other species and target materials, has shown weak dependences of the ejected velocity profiles on the ion energy and incidence angle<sup>13, 17-19, 24</sup>, but the variations are relatively small compared to our experimental uncertainty and the accuracy needed for engineering analyses.

#### IV. Conclusion

We have performed LIF measurements to determine the velocity profiles of sputtered boron atoms from BN targets due to bombardment by low energy Xe ions. In both cases, the measurements aid the linkage between number densities and fluxes (erosion rates) of sputtered particles. The LIF measurement scheme used a frequency-quadrupled continuous-wave ECDL system in the vicinity of 250 nm as the illumination source. Opto-galvanic spectroscopy has been applied to obtain the boron thermal absorption spectrum which acts as a frequency reference for the LIF spectra. The weak fluorescence signals from excited boron atoms have been amplified and measured with a lock-in amplifier. A validating measurement of pure boron yielded a surface binding energy ( $E_b=5.7±0.3$  eV) which agrees well with previous measurement results. The linearity of the fluorescence signal has also been confirmed. In addition to velocity measurements for higher energy Xe and Ar ions, we have now also performed measurements for Xe ions in the energy range of 100-300 eV yielding a surface binding energy of  $E_b=4.8±0.2$  eV.

## Acknowledgments

The authors thank Professor John D. Williams and Jim L. Topper for their technical contributions. The authors thank Professor Alec Gallimore (University of Michigan) for his ongoing collaboration in the development of CRDS erosion sensors for Hall thruster lifetime studies.

## References

1. J. R. Anderson, K. D. Goodfellow, J. E. Polk, R. F. Shotwell, V. K. Rawlin, J. S. Sovey, and M. J. Patterson, "Results of an On-going Long Duration Ground Test of the DS-1 Flight Space Engine," in *the 35th Joint Propulsion Conference*, (Los Angeles, CA, 1999) AIAA 99-2857.
2. C. E. Garner, J. R. Brophy, J. E. Polk, and L. C. Pless, "Performance Evaluation and Life Testing of the SPT-100," in *the 30th AIAA/SAE/ASME/ASEE Joint Propulsion Conference and Exhibit*, (Indianapolis, IN, 1994) AIAA-94-2856.
3. C. E. Garner, J. R. Brophy, J. F. Polk, and L. C. Pleass, "A 5730-Hr Cyclic Endurance Test of the SPT-100," in *the 24th IEPC*, (Moscow, 1995) IEPC-95-179.
4. V. Surla, P. J. Wilbur, M. Johnson, J. D. Williams, and A. P. Yalin, "Sputter erosion measurements of titanium and molybdenum by cavity ring-down spectroscopy," *Review of Scientific Instruments* **75**, 3025-3030 (2004)
5. A. P. Yalin, V. Surla, M. Butweiller, and J. D. Williams, "Detection of sputtered metals with cavity ring-down spectroscopy," *Applied Optics* **44**, 6496-6505 (2005)
6. V. Surla, and A. P. Yalin, "Differential sputter yield measurements using cavity ringdown spectroscopy," *Applied Optics* **46**, 3987-3994 (2007)
7. L. Tao, A. P. Yalin, and N. Yamamoto, "Cavity ring-down spectroscopy sensor for ion beam etch monitoring and end-point detection of multilayer structures," *Review of Scientific Instruments* **79**, (2008)
8. A. P. Yalin, L. Tao, R. Sullenberger, M. Oya, N. Yamamoto, T. B. Smith, and A. D. Gallimore, "High-Sensitivity Boron Nitride Sputter Erosion Measurements by Continuous-Wave Cavity Ring-Down Spectroscopy," in *the 44th AIAA/SAE/ASME/ASEE Joint Propulsion Conference and Exhibit*, (Hartford, CT, 2008) AIAA 2008-5091.
9. L. Tao, N. Yamamoto, A. D. Gallimore, and A. P. Yalin, "Development of a Cavity Ring-Down Spectroscopy Sensor for Boron Nitride Erosion in Hall Thrusters," in *the 31st International Electric Propulsion Conference*, (Ann Arbor, MI, 2009) *IEPC-2009-2147*.
10. N. Yamamoto, L. Tao, B. Rubin, J. D. Williams, and A. P. Yalin, "Sputter Erosion Sensor for Anode Layer-Type Hall Thrusters Using Cavity Ring-Down Spectroscopy," *Journal of Propulsion and Power* **26**, 142-148 (2010)
11. W. Huang, A. D. Gallimore, T. B. Smith, L. Tao, and A. P. Yalin, "Initial Cavity Ring-Down Density Measurement on a 6-kW Hall Thruster," in *47th AIAA Joint Propulsion Conference*, (San Diego, CA, 2011)
12. L. Tao, and A. P. Yalin, "LIF Velocity Measurement of Sputtered Boron Atoms from Boron Nitride Target," in *AIAA 46th Joint Propulsion Conference*, (Nashville, TN, 2010)
13. G. Betz, and K. Wien, "Energy And Angular-Distributions Of Sputtered Particles," *International Journal of Mass Spectrometry and Ion Processes* **140**, 1-110 (1994)
14. E. Pasch, P. Bogen, and P. Mertens, "Sputtering Of Amorphous C-H And C/B-H Layers By Argon Ions," *Journal of Nuclear Materials* **196**, 1065-1068 (1992)
15. M. Rowekamp, A. Goehlich, and H. F. Dobeles, "Diagnostics Of Sputtering Processes Of Carbon And Carbides By Laser-Induced Fluorescence Spectroscopy In The Vuv At 166-Nm," *Applied Physics a-Materials Science & Processing* **54**, 61-67 (1992)
16. Y. Ito, N. Nakano, T. Yoshidome, M. Isobe, and M. Nishikawa, "Spectroscopic measurement of kinetic energy of sputtered boron in electron cyclotron resonance plasma," *Journal of Nuclear Materials* **241**, 1122-1126 (1997)
17. M. J. Pellin, R. B. Wright, and D. M. Gruen, "Laser Fluorescence Spectroscopy Of Sputtered Zirconium Atoms," *Journal of Chemical Physics* **74**, 6448-6457 (1981)
18. C. E. Young, W. F. Calaway, M. J. Pellin, and D. M. Gruen, "Velocity And Electronic State Distributions Of Sputtered Fe Atoms By Laser-Induced Fluorescence Spectroscopy," *Journal of Vacuum Science & Technology a-Vacuum Surfaces and Films* **2**, 693-697 (1984)
19. H. L. Bay, "Laser-Induced Fluorescence As A Technique For Investigations Of Sputtering Phenomena," *Nuclear Instruments & Methods in Physics Research Section B-Beam Interactions with Materials and Atoms* **18**, 430-445 (1987)
20. T. R. Obrian, and J. E. Lawler, "Radiative Lifetimes In B-I Using Ultraviolet And Vacuum-Ultraviolet Laser-Induced Fluorescence," *Astronomy and Astrophysics* **255**, 420-426 (1992)
21. B. Rubin, J. L. Topper, and A. P. Yalin, "Total and differential sputter yields of boron nitride measured by quartz crystal microbalance," *Journal of Physics D-Applied Physics* **42**, (2009)
22. J. F. Ziegler, "SRIM-2008.04," (<http://www.srim.org>, Annapolis, MD, 2010).
23. E. Aheda, A. Anton, I. Garmendia, I. Caro, and J. Gonzalez del Amo, "Simulation of Wall Erosion in Hall Thrusters," in *the 30th International Electric Propulsion Conference*, (Florence, Italy, September 17-20, 2007) *IEPC-2007-2067*.
24. A. Goehlich, D. Gillmen, and H. F. Dobeles, "An Experimental Investigation of Angular Resolved Energy Distribution of Atoms Sputtered from Evaporated Aluminum Films," *Nuclear Instruments and Methods in Physics Research B*, pp. 351-363 (2001)